

Simulation Of Resonance Propagation With Grid Connected And Islanding Microgrids

¹Chintaguntla Anusha, ²Ch.Rami Reddy

¹M Tech, Nalanda Institute Of Engineering And Technology.

²Assistant professor, Nalanda Institute Of Engineering And Technology.

Abstract—In this paper, a microgrid resonance propagation model is investigated. To actively mitigate the resonance using DG units, an enhanced DG unit control scheme that uses the concept of virtual impedance is proposed. It can be seen that a conventional voltage-controlled dg unit with an LC filter has a short-circuit feature at the chosen harmonic frequencies, whereas a current-controlled dg unit presents an open-circuit characteristic. The application of underground cables and shunt capacitor banks may introduce power distribution system resonances. This paper additionally focuses on developing a voltage-controlled dg unit-based active harmonic damping technique for grid-connected and islanding microgrid systems. An improved virtual impedance control method with a virtual damping resistor and a nonlinear virtual capacitor is proposed. The nonlinear virtual capacitor is used to compensate the harmonic dip on the grid-side inductor of a dg unit LCL filter. The virtual resistance is principally answerable for microgrid resonance damping. The effectiveness of the proposed damping method is examined using each a single dg unit and multiple parallel dg units.

Index Terms—Active power filter, distributed power generation, droop control, grid-connected converter, microgrid, power quality, renewable energy system, resonance propagation, virtual impedance.

I. INTRODUCTION

The increasing application of nonlinear loads can lead to significant harmonic pollution in a power distribution system. The harmonic distortion might excite complicated resonances, particularly in power systems with underground cables or subsea cables and. In fact, these cables with nontrivial parasitic shunt capacitance will form an LC ladder network to amplify resonances. In order to mitigate system resonances, damping resistors or passive filters can be placed in the distribution networks. However, the mitigation of resonance propagation exploitation passive components is subject to some well understood problems, like power loss and additional investment. Moreover, a passive filter might even bring extra resonances if it's designed or installed without knowing detailed system configurations. To avoid the adoption of passive damping equipment, numerous types of active damping methods are developed.

Among them, the resistive active power filter (R-APF) is often considered as a promising way

to understand better performance. Conventionally, the principle of R-APF is to emulate the behavior of passive damping resistors by applying a closed-loop current-controlled method (CCM) to power electronics converters. In this management category, the R-APF will be simply modeled as a virtual harmonic resistor if it's viewed at the distribution system level. In addition, many changed R-APF ideas were additionally developed in the recent literature. In the separate tuning method was proposed to regulate damping resistances at different harmonic orders.

For current-controlled dg units, the auxiliary R-APF function can be seamlessly incorporated into the primary dg real power injection function by modifying the current reference. However, conventional CCM will hardly provide direct voltage support throughout microgrid islanding operation. To beat this limitation, an enhanced voltage-controlled method (VCM) was recently proposed for dg units with high-order LC or LCL filters. It can be seen that the control method in regulates the dg unit as virtual impedance, that is dependent on the present feeder electric resistance. Once the feeder electric resistance is inductive, this method could not provide enough damping effects to system resonance.

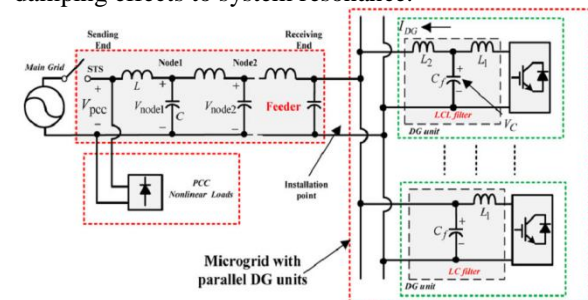


Fig. 1. Simplified one-line diagram of a single-phase microgrid service. Simulated results are provided to confirm the validity of the proposed method.

II. MODELING OF DG UNITS IN MICROGRID SYSTEM

Fig. 1 illustrates the configuration of a single-phase microgrid system, where a few dg units are interconnected to the point of common coupling (PCC) through an extended underground feeder. For the sake of simplicity, this paper only adopts an easy microgrid configuration to demonstrate how the microgrid power quality is affected by resonance

propagation. in addition, this paper also assumes that shunt capacitor banks and parasitic feeder capacitances are equally distributed in the feeder.

Note that the static transfer switch (STS) controls the operation mode of the microgrid. when the most grid is disconnected from the microgrid, the PCC nonlinear loads shall be supplied by the standalone dg units.

A. Distributed Parameter Model in Grid-Tied Operation

For a protracted feeder, as illustrated in Fig. 1, a lumped parameter model isn't able to describe its resonance propagation characteristics. alternatively, the distributed parameter model was mentioned in [3] and [6], where the voltage distortions at PCC induce a harmonic voltage standing wave on the feeders. where the kth PCC harmonic voltage is assumed to be stiff and $V_{pcck} \cdot V_k(x)$ and $I_k(x)$ square measure the feeder kth harmonic voltage and harmonic current at position x. The length of the feeder is l.

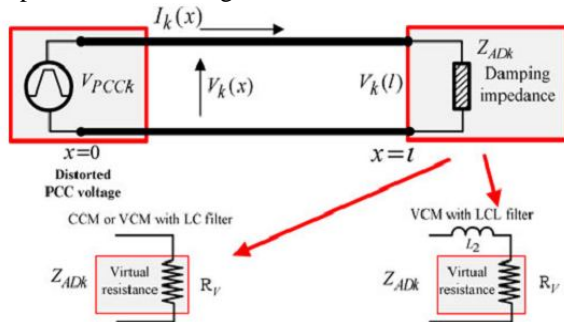


Fig. 2. Equivalent circuit of a single grid-connected DG unit at the kth harmonic frequency.

It is easy to obtain the harmonic voltage-current standing wave equations at the harmonic order k as

$$V_k(x) = Ae^{-\gamma x} + Be^{\gamma x} \quad (1)$$

$$I_k(x) = \frac{1}{z}(Ae^{-\gamma x} - Be^{\gamma x}) \quad (2)$$

where A and B are constants, which are determined by feeder boundary conditions. z and γ are the characteristics impedance [3] of the feeder without considering the line resistance as

$$Z = \sqrt{\frac{L}{C}} \quad (3)$$

$$\gamma = jk\omega_f \sqrt{LC} \quad (4)$$

where ω_f is the fundamental angular frequency and L and C are the feeder equivalent inductance and shunt capacitance per kilometer, respectively.

1) DG Units with CCM and R-APF Control: To determine the boundary conditions of the feeder, the equivalent harmonic impedance (Z_{ADk}) of the DG unit must be derived. First, the current reference (I_{ref}) of a CCM-based DG unit can be obtained as

$$I_{ref} = i_{reff} - I_{AD} = I_{reff} - \frac{H_D(s) \cdot V(l)}{R_V} \quad (5)$$

where I_{reff} is the fundamental current reference for DG unit power control, I_{AD} is the harmonic current reference for system resonance compensation, $V(l)$ is the measured installation point voltage at the receiving end of the feeder, $H_D(s)$ is the transfer function of a harmonic detector, which extracts the harmonic components of the installation point voltage, and R_V is the command virtual resistance.

$$\omega_{DG} = \omega_f + D_p \cdot (P_{ref} - P_{LPF}) \quad (6)$$

$$E_{DG} = E + D_q \cdot (Q_{ref} - Q_{LPF}) + \frac{K_Q}{S} (Q_{ref} - Q_{LPF}) \quad (7)$$

where ω_f and ω_{DG} are the nominal and reference angular frequencies. E and E_{DG} are the nominal and reference DG voltage magnitudes. P_{LPF} and Q_{LPF} are the measured power with lowpass filtering. D_p and D_q are the droop slopes of the controller.

Note that with the integral control to regulate DG unit voltage magnitude in (7), the steady-state reactive power control error at the grid-tied operation is zero. Once the voltage magnitude reference and the frequency reference are determined, the ripple-free instantaneous voltage reference (V_{reff}) can be easily obtained. The equivalent impedance of VCM-based DG unit with an LC filter has already been tuned to be resistive, by adding a DG line current (I_{DG}) feed-forward term to the voltage control reference. Although previous VCM-based DG equivalent impedance shaping techniques mainly focus on improving the power sharing performance of multiple DG units in an islanding microgrid, similar idea can also be used to mitigate the harmonic propagation along the feeder as

$$V_{ref} = V_{reff} - V_{AD} = V_{reff} - R_V \cdot (H_D(s) \cdot I_{DG}) \quad (8)$$

where V_{reff} is the fundamental voltage reference derived from droop control in (6) and (7), V_{AD} is the harmonic voltage reference for DG unit harmonic impedance shaping, I_{DG} is the measured DG unit line current (see Fig. 1), $H_D(s)$ is the transfer function of a harmonic detector, which extracts the harmonic components of DG unit line current, and R_V is the virtual resistance command. Since a grid-connected DG unit using either CCM or VCM can be modeled by an equivalent harmonic impedance at the receiving end of the feeder, the following boundary conditions can be obtained:

$$\frac{V_k(l)}{I_k(l)} = Z_{ADk} \quad (9)$$

$$V_k(0) = V_{PCCk} \quad (10)$$

By solving (1), (2), (9), and (10), the harmonic voltage propagation at the harmonic order k can be expressed as

$$V(x)_k = \frac{Z_{ADK} \cos h(\gamma(l-x)) + z \sin h(\gamma(l-x))}{Z_{ADK} \cos h(\gamma l) + z \sin h(\gamma l)} V_{PCCk} \quad (11)$$

With the obtained equation in (11), the impact of DG active damping scheme to the harmonic voltage propagation along the feeder can be easily analyzed. Note that when the microgrid feeder is purely RL impedance, the DG unit can still work as a virtual harmonic resistor at the end of the feeder. In this case, the DG unit has the capability of absorbing some PCC nonlinear load current if it is designed and controlled properly

B. Distributed Parameter Model in Islanding Operation

The previous section focuses on the analysis of grid-tied DG units. For an islanding microgrid system, the VCM operation of DG units is needed for direct voltage support. To the best of the authors' knowledge, the quantitative analysis of islanding microgrid harmonic propagation is not available. When only a single DG unit is placed in the islanding system, constant voltage magnitude and constant frequency (CVMCF) control can be used.

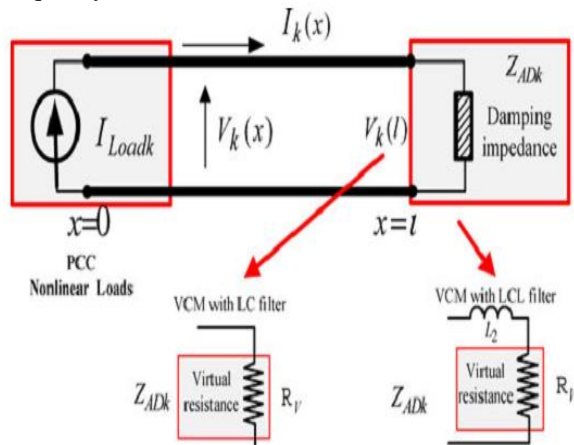


Fig. 3. Equivalent circuit of a single islanding DG unit at the kth harmonic frequency.

On the other hand, for the operation of multiple DG units in the microgrid (see Fig. 1), the droop control method in (6) and (7) [by setting $KQ = 0$ in (7)] shall be employed to realize proper power sharing among these DG units. Considering the focus of this section is to investigate the harmonic voltage damping in a stand-alone islanding system, a single DG unit at the receiving end of the feeder is considered. The circuit model of an islanding system at the harmonic order k is illustrated in Fig. 3, With the knowledge of boundary conditions at both sending and receiving ends as

$$I_k(0) = I_{Loadk} \quad (12)$$

$$\frac{V_k(l)}{I_k(l)} = Z_{ADK} \quad (13)$$

The kth harmonic voltage distortion along the feeder can be obtained

$$V_k(x) = \left(\frac{e^{-\gamma x}}{1 + ((z - Z_{ADK}) / (z + Z_{ADK})) e^{2\gamma l}} - \frac{e^{\gamma x}}{1 + ((z + \frac{Z_{ADK}}{z - Z_{ADK}})) z I_{Load}} \right) \quad (14)$$

From (14), it can be noticed that the voltage propagation in an islanding system harmonic is also related to the DG-unitequivalent harmonic impedance. In order to maintain satisfied voltage quality, the equivalent harmonic impedance of islanding DG units shall also be properly designed.

III. EVALUATION OF DAMPING PERFORMANCE

In this section, the performance of VCM-based DG units at different operation modes is investigated.

A. Evaluation of a Single DG Unit at the End of the Feeder

1) Grid-Tied Operation: first, the performance of a grid-tied dg unit with an LCL filter is investigated. The system parameters area unit listed in Table I. Fig. 4 shows harmonic voltage distortions on a 6 kilometer feeder. The harmonic voltage distortion issue here is normalized to the voltage distortions at PCC as $V(x)_k / V_{PCCk}$. when the conventional VCM while not damping is applied to the dg unit, the LCL filter condenser voltage is ripple free and the dg unit works as an inductor (L_2) at the harmonic frequencies.

TABLE I
FEEDER PARAMETERS

System parameter	value
Feeder length	6km
Number of diodes	7
Line Inductor L	1mH/km
Capacitance C	20 μ F/km
DG unit parameter	Value
With LCL filter	L1=2mH L2=3.5mH Cf=20 μ F
Command virtual resistance	RV=5.5 ω

It is seen that the feeder is sensitive to seventh harmonic voltage distortion at the PCC. once the dg unit is controlled by the changed voltage control reference as shown in (8), it works as an equivalent RL impedance at the receiving end of the feeder. consequently, the most obvious seventh harmonic voltage propagation is effectively reduced as shown in Fig. 4(c). once a metric weight unit is coupled to the distribution system with an LC filter, the dg unit is like a harmonic damping resistor by the control scheme in (8). The corresponding performance of the system at different harmonic orders is additionally investigated in Fig. 4.

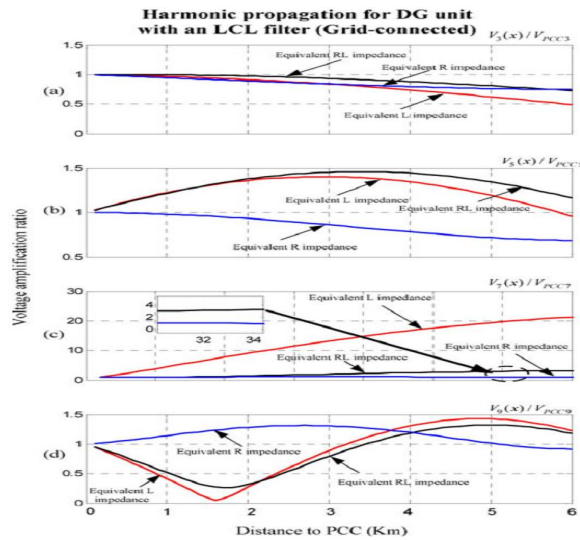


Fig. 4. Harmonic voltage amplification in a single DG unit grid-connected operation [(a)–(d): amplification ratio at 3rd, 5th, 7th, and 9th harmonic frequencies].

Therefore, the obtained waveforms can be used to evaluate the performance of CCM-based DG units in a similar way. 2) Stand-alone Operation: In addition, a DG unit with an LCL filter in a standalone islanding system is also examined. In contrast to the performance during grid-tied operation, the voltage distortion at PCC is not stiff in this case and it is dependent on the harmonic current from the PCC nonlinear loads. As a result, the harmonic voltage amplification factor $V(x)_k/V_{PCCk}$ that is used in grid-tied systems is not very appropriate for an islanded system. Alternatively, the feeder harmonic voltage over PCC load harmonic current ($V_k(x)/V_{Loadk}$) can be used to describe the harmonic propagation characteristic of the system. The associated harmonic propagation performance is obtained in Fig. 5

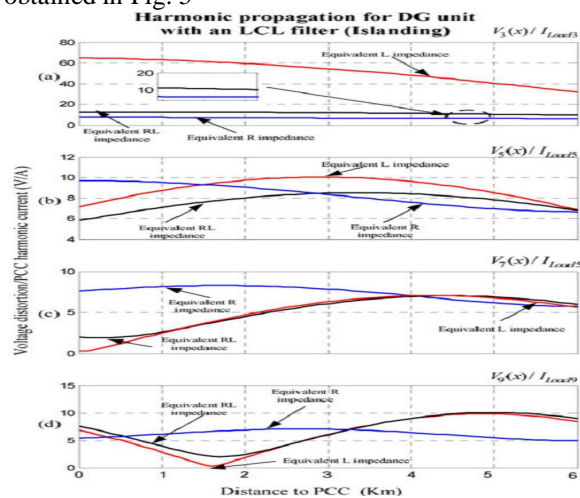


Fig. 5. Harmonic voltage amplification in a single DG unit islanding operation [(a)–(d): amplification ratio at 3rd, 5th, 7th, and 9th harmonic frequencies].

B. Evaluation of Multiple DG Units at the End of the Feeder

The performance of a microgrid with multiple dg units is increasingly discussed in the recent literature. In addition to achieve correct power sharing among multiple dg units, realizing superior harmonic damping performance in a cooperative manner is also attractive. For parallel dg units as shown in Fig. 1, they shall share the active damping current according to their respective power rating [4].

To modify the discussion, 2 VCM controlled dg units at a similar power rating are used to equally share the harmonic current associated with the active damping control. If the dg unit with an LC filter is controlled as a harmonic damping resistor R whereas the other one with an LCL filter is regulated because the RL damping ohmic resistance, the corresponding circuit diagram at the harmonic order k may be illustrated in Fig. 6.

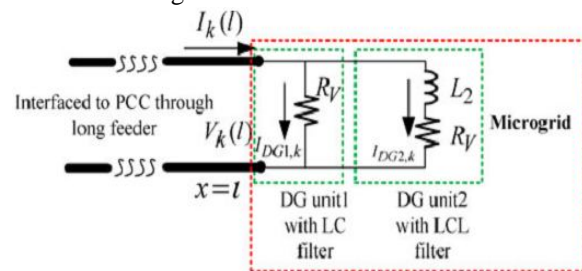


Fig. 6. Circuit diagram of a double-DG-based microgrid at the k th harmonic frequency

For a microgrid with two DG units, as shown in Fig. 6, its equivalent impedance is the parallel equivalent impedance of parallel DG units as

$$Z_{ADK,microgrid} = \frac{Z_{ADK,DG1} \cdot Z_{ADK,DG2}}{Z_{ADK,DG1} + Z_{ADK,DG2}} \quad (15)$$

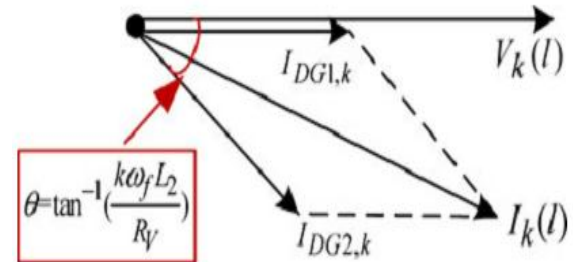


Fig. 7. Phasor diagram of the harmonic circulating current among parallel DG units.

IV. REALIZATION OF VIRTUAL DAMPING IMPEDANCE THROUGH DG VOLTAGE CONTROL

It has been clarified that an LCL filter grid-side inductor (L_2) can affect the performance of distribution system harmonic suppression, especially in the case of multiple DG units. In order to compensate the impact of LCL filter grid-side inductor, the harmonic voltage damping scheme as shown in (8) shall be further improved.

A. Conventional Voltage Tracking

First, a negative virtual inductor can be produced by VCM. Accordingly, the modified voltage reference is obtained as

$$\begin{aligned} V_{ref} &= V_{reff} - V_{AD} - V_{comp} \\ V_{ref} &= R_V - H_D(s) \cdot I_{DG} - s(-L_2) \cdot H_D(s) \cdot I_{DG} \end{aligned} \quad (16)$$

By further looking into (16), one can find that the implementation of virtual inductor involves derivative operation, which may adversely amplify system background noises. For instance, if a band-stop filter is selected to filter out the fundamental components as

$$H_D(s) = 1 - \frac{2\omega_{BP}S}{s^2 + 2\omega_{BP}S + \omega_f^2} \quad (17)$$

where ω_{BP} is the cutoff bandwidth of the band-stop filter, the voltage compensation term V_{Comp} in (16) can be expressed as

$$V_{comp} = S(-L_2) \cdot H_D(s) I_{DG} = \left(-sL_2 + \frac{2\omega_{BP}L_2S^2}{s^2 + 2\omega_{BP}S + \omega_f^2} \right) \cdot I_{DG} \quad (18)$$

The diagram of a DG unit with negative virtual inductor control is shown in Fig. 8. As illustrated, the DG unit is interfaced to long feeder with an LCL filter.

B. Implementation of Nonlinear Virtual Capacitor

In this subsection, a well-understood double-loop voltage controller is selected for DG unit voltage tracking. In the outer filter capacitor voltage control loop, the proportional and multiple resonant (PR) controllers are used as

$$\begin{aligned} I_{inner} &= G_{outer}(s) \cdot (V_{ref} - V_C) = \\ &\left(K_p + \sum_K \frac{2k_{ik}\omega_{ck}^2}{s^2 + 2\omega_{ck}k^2 + (k\omega_f)^2} \right) \cdot (V_{ref} - V_C) \end{aligned} \quad (19)$$

where K_P is the outer loop proportional gain, K_{ik} is the gain of resonant controller at fundamental and selected harmonic frequencies, ω_{ck} is the cutoff bandwidth, and I_{inner} is the control reference for the inner control loop. In the inner loop controller ($G_{inner}(s)$), a simple proportional controller (K_{inner}) is employed and the inverter output current (I_{inv}) is measured as the feedback.

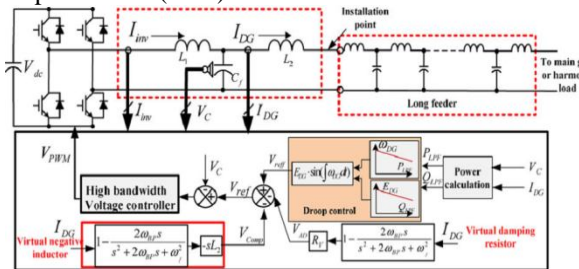


Fig. 8. Mitigation of distribution feeder harmonic propagation using virtual resistor and virtual negative inductor

This is because the impedance of a capacitor also has 90° lagging phase angle, which is the same as that in a negative inductor.

$$L_2(\omega ft) - \frac{1}{C_{vk}(\omega ft)} = 0 \quad (20)$$

Where ω is the fundamental angular frequency and C_v is the command capacitance at the harmonic order t .

TABLE II
DG UNIT PARAMETERS

Control parameter	Value
Rated voltage	RMS 60V
Rated frequency	F=60Hz
Droop coefficients	Dp=1/300; Dp=1/300;KQ=1/30
Proportional gain	Kp1=0.11
Resonant gain	Kif=20, Ki3=15, Ki5=15, Ki9=10;
Cutoff frequency	$\omega_{ck}=4$ rad/s(K=f,3,5,7 and 9)
Inner loop controller	$K_{inner}=20$
DC link voltage	$V_{dc}=240$ v
Sampling and Switching frequency	12KHZ
Circuit parameter	Value
LCL filter	L1=2mH L2=3.5mH Cf=20 μ F
LC filter	L1=2mH L2=0mH Cf=20 μ F(DG unit 1 in Figs. 14 and 15)
Command virtual resistance	$R_V=5.5\omega$ (DG unit in Figs. 10-13) $R_V=11\omega$ (DG unit 1 and DG unit 2 in Figs.14 and 15)

Afterwards, the voltage drops on the nonlinear virtual capacitor can be obtained as

$$\begin{aligned} V_{comp} &= \sum_t \frac{1}{sC_{vt}} \cdot I_{DGt} \\ &= \sum_t \frac{1}{sC_{vt}} \cdot (H_{Dt}(s) \cdot I_{DGt}) \end{aligned} \quad (21)$$

Where $H_{Dt}(s)$ is the harmonic detector to detect the t th DG harmonic current I_{DGt} . It can also be seen that parallel resonant controllers used in the outer loop voltage control in (19) are essentially a set of band-pass filters with narrow bandwidth ω_{ck} and amplified magnitudes K_{ik} . Indeed, the harmonic selective capability has already been embedded in the resonant controllers.

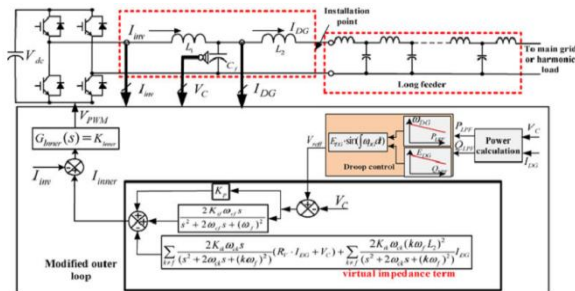


Fig. 9. Mitigation of harmonic propagation using virtual resistor and nonlinear virtual capacitor.

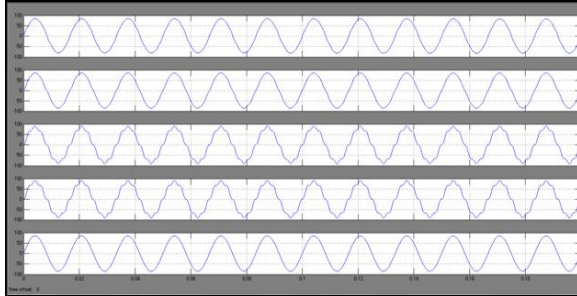


Fig. 10. Harmonic voltage amplification during a single DG unit gridconnected operation (without damping) [from upper to lower: (a) PCC voltage (THD = 4.0%); (b) node 1 voltage (THD = 4.56%); (c) node 3 voltage (THD = 10.91%); (d) node 5 voltage (THD = 12.59%); (e) DG unit filter capacitor voltage (THD = 0.38%)].

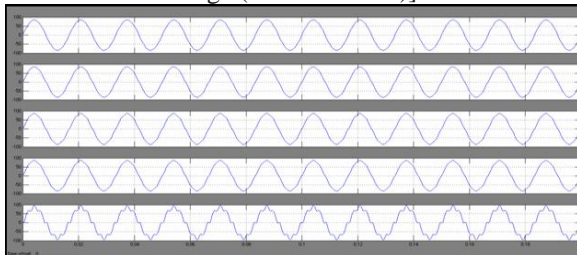


Fig. 11. Harmonic voltage amplification during a single DG unit gridconnected operation (with virtual nonlinear capacitor and resistor based active damping) [from upper to lower: (a) PCC voltage (THD = 4.0%); (b) node 1 voltage (THD = 4.1%); (c) node 3 voltage (THD = 3.7%); (d) node 5 voltage (THD = 3.2%); and (e) DG unit filter capacitor voltage (THD = 5.4%)].

V. VERIFICATION RESULTS

Simulated results have been obtained from a single-phase low voltage microgrid. To emulate the behavior of six kilometers feeder with distributed parameters, a DG unit with an LCL filter is connected to PCC through a ladder network with six identical LC filter units (see Fig. 1).

Single DG Unit Grid-Tied Operation

At first, the performance of a grid-connected DG unit with an LCL filter is examined. The PCC voltage in this simulation is stiff and it has 2.0% distortion at each lower order harmonic frequency (3rd, 5th, 7th, and 9th harmonics).

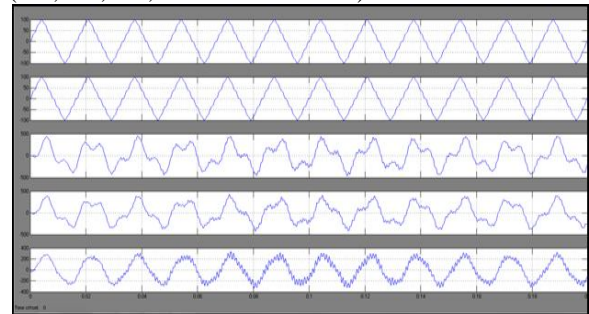


Fig. 14. Harmonic voltage amplification during a single DG unit islanding operation (without damping) [from upper to lower: (a) PCC voltage (THD = 15.2%); (b) node 1 voltage (THD = 14.7%); (c) node 3 voltage (THD = 11.9%); (d) node 5 voltage (THD = 10.5%); and (e) DG unit filter capacitor voltage (THD = 1.6%)].

TABLE II
HARMONIC SPECTRUM OF A GRID-CONNECTED MICROGRID WITHOUT ACTIVE DAMPING
(CORRESPONDING TO FIG. 10)

	3 rd harmonic	5 th harmonic	7 th harmonic	9 th harmonic	11 th harmonic	13 th harmonic	THD
PCC voltage	2.00%	2.00%	2.00%	2.00%	0%	0%	4.00%
Node 1 Voltage	1.91%	2.41%	2.89%	1.31%	0.05%	0.03%	4.56%
Node 3 Voltage	1.65%	2.92%	10.37%	0.74%	0.03%	0.04%	10.91%
Node 5 Voltage	1.24%	2.57%	12.31%	2.07%	0.01%	0.02%	12.59%
DG voltage	0.02%	0.04%	0.10%	0.14%	0.15%	0.2%	0.38%

TABLE III
HARMONIC SPECTRUM OF AN ISLANDING MICROGRID WITHOUT ACTIVE DAMPING
(CORRESPONDING TO FIG. 12)

	3 rd harmonic	5 th harmonic	7 th harmonic	9 th harmonic	11 th harmonic	13 th harmonic	THD
PCC voltage	13.19%	2.95%	0.29%	1.66%	6.58%	0.54%	15.19%
Node 1 Voltage	11.96%	3.68%	0.39%	1.07%	6.62%	1.46%	14.67%
Node 3 Voltage	10.05%	4.35%	1.45%	0.66%	1.09%	0.61%	11.93%
Node 5 Voltage	7.54%	3.83%	1.73%	1.76%	5.98%	0.86%	10.51%
DG voltage	0.10%	0.05%	0.02%	0.45%	1.43%	0.2%	1.60%

TABLE IV
DG UNIT PARAMETERS

Control parameter	Value
Rated voltage	RMS 60V
Rated frequency	F=60Hz
Droop coefficients	$D_p=1/300$; $D_p=1/300$; $K_Q=1/30$
Proportional gain	$K_p=0.11$
Resonant gain	$K_{if}=20, K_{i3}=15, K_{i5}=15, K_{i9}=10$;
Cutoff frequency	$\omega_{ck}=4$ rad/s($K=f, 3, 5, 7$ and 9)
Inner loop controller	$K_{inner}=20$
DC link voltage	$V_{dc}=240$ v
Sampling and Switching frequency	12KHZ
Circuit parameter	Value
LCL filter	$L_1=2$ mH $L_2=3.5$ mH $C_f=20$ μ F
LC filter	$L_1=2$ mH $L_2=0$ mH $C_f=20$ μ F(DG unit 1 in Figs. 14 and 15)
Command virtual resistance	$R_v=5.5\omega$ (DG unit in Figs. 10-13) $R_v=11\omega$ (DG unit 1 and DG unit 2 in Figs.14 and 15)

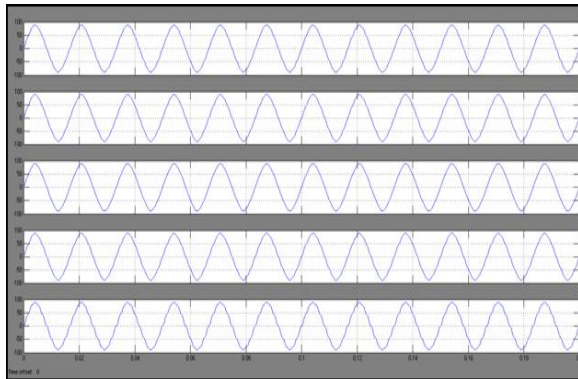


Fig. 15. Harmonic voltage amplification during a single DG unit islanding operation (with virtual nonlinear capacitor and resistor based active damping) [from upper to lower: (a) PCC voltage (THD = 6.1%); (b) node 1 voltage (THD = 6.0%); (c) node 3 voltage (THD = 5.2%); (d) node 5 voltage (THD = 5.3%); and (e) DG unit filter capacitor voltage (THD = 7.1%)].

A. Single DG Unit Islanding Operation

In addition to grid-connected operation, the performance of a single DG unit in islanding operation is also investigated. In this case, the PCC lad is a single-phase diode rectifier and it is supplied by the DG unit through long feeder. When the conventional VCM without damping is adopted, the performance of the system is obtained in Fig. 12. Similar to the grid-tied operation, the voltage waveforms at PCC, nodes 1, 3, and 5, and DG unit filter capacitor are shown from channels (a) to (e), respectively.

B. Multiple DG Units Grid-Tied Operation

To verify the circulating harmonic current between multiple DG units, two grid-connected DG

units at the same power rating are placed at the receiving end of the feeder.

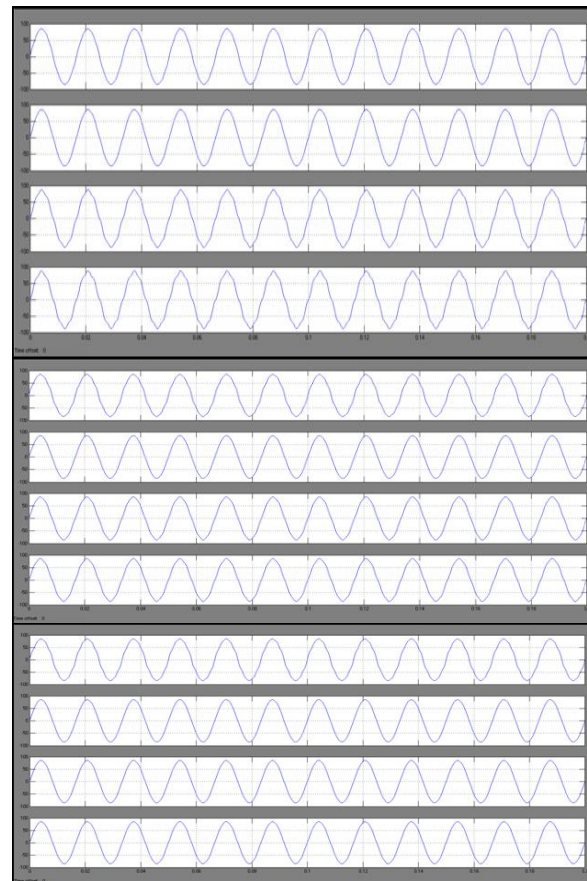


Fig. 16. Harmonic voltage amplification along the feeders (grid-tied operation of two parallel DG units).

VI. CONCLUSION

In this paper, the impacts of voltage-controlled and current-controlled distributed

generation (DG) units to microgrid resonance propagation are compared. To actively mitigate the resonance using DG units, an enhanced DG unit component of the proposed nonlinear virtual impedance is employed to compensate the impact of dg unit LCL filter grid-side inductor. The resistive element is responsible for active damping. With properly controlled dg equivalent harmonic impedance at chosen harmonic frequencies, the proposed method can even eliminate the harmonic circulating current among multiple dg units with mismatched output filter parameters. Here we are using the fuzzy controller compared to other controllers due to its accurate performance. Comprehensive simulations are conducted to substantiate the validity of the proposed method.

REFERENCES

- [1] H. Akagi, "Active harmonic filters," *Proc. IEEE*, vol. 93, no. 12, pp. 2128–2141, Dec. 2005. [2] H. Akagi, H. Fujita, and K. Wada, "A shunt active filter based on voltage detection for harmonic termination for radial power distribution system," *IEEE Trans. Ind. Appl.*, vol. 35, no. 4, pp. 682–690, Jul./Aug. 1995.
- [3] K. Wada, H. Fujita, and H. Akagi, "Consideration of a shunt active filter based on voltage detection for installation on a long distribution feeder," *IEEE Trans. Ind. Appl.*, vol. 38, no. 4, pp. 1123–1130, Jul./Aug. 2002.
- [4] P.-T. Cheng and T.-L. Lee, "Distributed active filter systems (DAFSs): A new approach to power system harmonics," *IEEE Trans. Ind. Appl.*, vol. 42, no. 5, pp. 1301–1309, Sep./Oct. 2006.
- [5] T.-L. Lee and P.-T. Cheng, "Design of a new cooperative harmonic filtering strategy for distributed generation interface converters in an islanding network," *IEEE Trans. Power Electron.*, vol. 42, no. 5, pp. 1301–1309, Sep. 2007.
- [6] T.-L. Lee, J.-C. Li, and P.-T. Cheng, "Discrete frequency-tuning active filter for power system harmonics," *IEEE Trans. Power Electron.*, vol. 24, no. 5, pp. 1209–1217, Apr. 2009.
- [7] T.-L. Lee and S.-H. Hu, "Discrete frequency-tuning active filter to suppress harmonic resonances of closed-loop distribution power system," *IEEE Trans. Power Electron.*, vol. 26, no. 1, pp. 137–148, Dec. 2010.
- [8] N. Pogaku and T. C. Green, "Harmonic mitigation throughout a distribution system: A distributed-generator-based solution," *IEE Proc. Gener. Transmiss. Distrib.*, vol. 153, no. 3, pp. 350–358, May 2006.
- [9] C. J. Gajanayake, D. M. Vilathgamuwa, P. C. Loh, R. Teodorescu, and F. Blaabjerg, "Z-source-inverter-based flexible distributed generation system solution for grid power quality improvement," *IEEE Trans. Energy Convers.*, vol. 24, pp. 695–704, Sep. 2009.
- [10] Y. W. Li, D. M. Vilathgamuwa, and P. C. Loh, "Design, analysis and realtime testing of a controller for multibus microgrid system," *IEEE Trans. Power Electron.*, vol. 19, no. 5, pp. 1195–1204, Sep. 2004.
- [11] Q.-C. Zhong and G. Weiss, "Synchronverters: Inverters that mimic synchronous generators," *IEEE Trans. Ind. Electron.*, vol. 58, no. 4, pp. 1259–1267, Apr. 2011.
- [12] J. He and Y. W. Li, "Analysis, design and implementation of virtual impedance for power electronics interfaced distributed generation," *IEEE Trans. Ind. Appl.*, vol. 47, no. 6, pp. 2525–2538, Nov./Dec. 2011.
- [13] Y. W. Li and C. N. Kao, "An accurate power control strategy for power electronics-interfaced distributed generation units operating in a low voltage multibus microgrid," *IEEE Trans. Power Electron.*, vol. 24, no. 12, pp. 2977–2988, Dec. 2009.
- [14] J. M. Guerrero, L. G. Vicuna, J. Matas, M. Castilla, and J. Miret, "Output impedance design of parallel-connected UPS inverters with wireless load sharing control," *IEEE Trans. Ind. Electron.*, vol. 52, no. 4, pp. 1126–1135, Aug. 2005.
- [15] J. M. Guerrero, L. G. Vicuna, J. Matas, M. Castilla, and J. Miret, "A wireless controller to enhance dynamic performance of parallel inverters in distributed generation systems," *IEEE Trans. Power Electron.*, vol. 19, no. 4, pp. 1205–1213, Sep. 2004.
- [16] J. M. Guerrero, J. C. Vasquez, J. Matas, L. G. de Vicuna, and M. Castilla, "Hierarchical control of droop-controlled AC and DC microgrids - A general approach toward standardization," *IEEE Trans. Ind. Electron.*, vol. 55, no. 1, pp. 158–172, Jan. 2011.